A compressive gammachirp auditory filter for both physiological and psychophysical data

Toshion Irino[a)]
NTT Communication Science Laboratories, 2-4, Hikaridai, Seika-cho, Soraku-gun, Kyoto 619-0237, Japan

Roy D. Patterson[b)]
Centre for Neural Basis of Hearing, Department of Physiology, University of Cambridge, Downing Street, Cambridge CB2 3EG, United Kingdom

(Received 13 October 2000; revised 17 January 2001; accepted 5 March 2001)

A gammachirp auditory filter was developed by Irino and Patterson [J. Acoust. Soc. Am. **101**, 412–419 (1997)] to provide a level-dependent version of the linear, gammatone auditory filter, with which to explain the level-dependent changes in cochlear filtering observed in psychophysical masking experiments. In this 'analytical' gammachirp filter, the chirp varied with level and there was no explicit representation of the change in filter gain or compression with level. Subsequently, Carney *et al.* [J. Acoust. Soc. Am. **105**, 2384–2391 (1999)] reviewed Carney and Yin's [J. Neurophysiol. **60**, 1653–1677 (1988)] reverse-correlation (revcor) data and showed that the frequency glide of the chirp does not vary with level in their data. In this article, the architecture of the analytical gammachirp is reviewed with respect to cochlear physiology and a new form of gammachirp filter is described in which the magnitude response, the gain, and the compression vary with level but the chirp does not. This new 'compressive' gammachirp filter is used to fit the level-dependent revcor data reported by Carney *et al.* (1999) and the level-dependent masking data reported by Rosen and Baker [Hear. Res. **73**, 231–243 (1994)]. © *2001 Acoustical Society of America.* [DOI: 10.1121/1.1367253]

PACS numbers: 43.64.Bt, 43.66.Dc [LHC]

I. INTRODUCTION

The gammatone auditory filter was developed by Boer (1975) and de Boer and de Jongh (1978) to describe cochlear impulse responses measured in cats with the reverse-correlation, or revcor, technique. The envelope of the impulse response was approximated with the gamma distribution from statistics; the carrier, or fine structure, of the impulse response was a sinusoid, or tone, at the center frequency of the filter (Johannesma, 1972). Carney and Yin (1988) fitted the gammatone to the data from more than 150 primary auditory fibers over a wide range of stimulus levels, and showed that it provided a good approximation to these impulse response data. At about the same time, Schofield (1985) reported that the magnitude response of the gammatone filter could explain the masking data gathered by Patterson (1976) to derive the shape of the auditory filter psychophysically. Patterson *et al.* (1992) then reported that when the order of the gammatone was four, there was good agreement between the magnitude response of the gammatone filter and the rounded exponential, or roex, auditory filter used to fit a wide range of human masking data by a number of modelers (for a review, see Patterson and Moore, 1986). In essence, this meant that if one made the reasonable assumption that the roex auditory filter had a minimum phase characteristic, then it would be equivalent to a gammatone auditory filter. Slaney (1993), Cooke (1993) and Patterson *et al.* (1995) extended the mathematical framework of the gammatone filter family, and described methods for constructing a range of gammatone filterbanks for use in auditory modeling.

A. Level dependence

Psychophysical measurements of the auditory filter shape (e.g., Lutfi and Patterson, 1984; Rosen and Baker, 1994) indicate that the filter is approximately symmetric in frequency at low stimulus levels, but it becomes asymmetric as stimulus level increases with the low-frequency skirt becoming much shallower than the high-frequency skirt at high stimulus levels. These findings are consistent with physiological observations of basilar membrane motion (e.g., Pickles, 1988; Ruggero, 1992). The original versions of the gammatone filter were linear and so they could not account for level-dependent changes in filter shape. Carney (1993) introduced level-dependent gain and bandwidth into an extended version of the gammatone with feedback, but it had a symmetric frequency response. Lyon (1996, 1997) developed a one-zero version of the gammatone filter to introduce asymmetry in frequency; he reduced the zeros in an IIR version of the gammatone filter (Slaney, 1993) leaving just one at zero to raise the low-frequency tail of the filter. Irino and Patterson (1997) developed a level-dependent gamma*chirp* auditory filter to accommodate the level-dependent asymmetry observed in human masking data (Lutfi and Patterson, 1984; Moore and Glasberg, 1987; Moore *et al.*, 1990; Rosen and Baker, 1994). In this analytic gammachirp, the rate of chirp, or frequency modulation, at the start of the impulse response varies with level as the asymmetry varies with level.

About the same time, de Boer and Nuttal (1997) and

[a)]Electronic mail: irino@cslab.kecl.ntt.co.jp
[b)]Electronic mail: roy.patterson@mrc-cbu.cam.ac.uk

Recio *et al.* (1998) extended measurements of the glide, or chirp, in the instantaneous frequency (IF) of the impulse response of the basilar membrane, originally discovered by Møller and Nilsson (1979). The trajectories of the IF glides resemble the glide in the gammachirp filter which was initially introduced to explain the psychophysical masking data. Subsequently, Carney *et al.* (1999) reanalyzed the revcor functions of Carney and Yin (1988) and showed that the instantaneous frequency did, indeed, chirp. The results were somewhat surprising, however, because the trajectory of the instantaneous frequency was not level dependent (see also de Boer and Nuttal, 2000). This was inconsistent with the level-dependent chirp described by Irino and Patterson (1997) when fitting human masking data with the analytical gammachirp filter. The problem arose because Irino and Patterson chose the simplest form of gammachirp that would enable them to make the gammatone level dependent, without regard for the constraints implied by cochlear physiology. Moreover, the simplest form of gammachirp cannot account for the level-dependent gain and compression observed physiologically around the peak frequency (Pickles, 1988; Recio *et al.*, 1998). To overcome these problems, Irino and Patterson (2000) have developed a modified version of the gammachirp filter in which there are explicit changes in gain and compression with level, but no change in the chirp with level as required by the revcor data of Carney *et al.* (1999).

The purpose of this article is to extend the domain of this compressive gammachirp auditory filter, and demonstrate that it can explain the level dependent effects observed in both psychophysical and physiological data within a unified filtering framework. In Sec. II we describe the analytic and compressive gammachirp filters; in Sec. III we describe the fit to the physiological revcor data (Carney *et al.*, 1999); and in Sec. IV we describe the fit to the human masking data (Rosen and Baker, 1994).

II. GAMMACHIRP AUDITORY FILTERS

This section presents (a) the mathematical background of the gammachirp filter, (b) the modification of the analytic gammachirp into the compressive gammachirp filter, and (c) how these filters are used to fit the data in Secs. III and IV.

A. Analytic gammachirp

The analytic, complex form of the gammachirp auditory filter (Irino and Patterson, 1997) is

$$g_{ca}(t) = a t^{n_1-1} \exp(-2\pi b_1 \mathrm{ERB}(f_{r1}) t) \times \exp(j 2\pi f_{r1} t + j c_1 \ln t + j\phi_1), \quad (1)$$

where time $t>0$; a is the amplitude; n_1 and b_1 are parameters defining the envelope of the gamma distribution; c_1 is the chirp factor; f_{r1} is the asymptotic frequency; $\mathrm{ERB}(f_{r1})$ is the equivalent rectangular bandwidth (Glasberg and Moore, 1990); ϕ_1 is the initial phase; and $\ln t$ is the natural logarithm of time. When $c_1=0$, Eq. (1) reduces to the complex impulse response of the gamma*tone* filter (Patterson *et al.*, 1995). The gammachirp filter in Eq. (1) was derived analytically, as the function satisfying minimum uncertainty constraints in the space of the Mellin transform (Irino and Patterson, 1997), and so it is referred to as an analytic gammachirp.

The instantaneous frequency $f_i(t)$ is the derivative of the phase function in Eq. (1); that is

$$f_i(t) = f_{r1} + c_1/t. \quad (2)$$

It is a function of time and it asymptotes to the frequency, f_{r1}, as t becomes large. The trajectory of the instantaneous frequency towards f_{r1} is an upchirp when $c_1<0$ and a downchirp when $c_1>0$. When $c_1=0$, Eq. (1) is the complex form of the gammatone filter.

The Fourier magnitude spectrum of Eq. (1) is

$$|G_{CA}(f)| = a_\Gamma \cdot |G_T(f)| \cdot \exp(c_1 \theta_1), \quad (3)$$

$$\theta_1 = \arctan\left(\frac{f-f_{r1}}{b_1 \mathrm{ERB}(f_{r1})}\right). \quad (4)$$

The first factor of the right hand-side of Eq. (3), a_Γ, is the amplitude and the second factor, $|G_T(f)|$, is the Fourier magnitude spectrum of the gammatone filter. The detailed forms of these factors are described in Appendix A. The third factor in Eq. (3), $\exp(c_1\theta_1)$, is an asymmetric function since θ_1 is an antisymmetric function centered at the asymptotic frequency, f_{r1} as shown in Eq. (4). This factor applies asymmetry to the gammatone and converts the composite frequency response into that of a gammachirp auditory filter. The asymmetric function is a low-pass filter when $c_1<0$, a high-pass filter when $c_1>0$, and unity when $c_1=0$. The peak, or best, frequency can be obtained from the derivative of Eq. (3) and it is

$$f_{p1} = f_{r1} + c_1 b_1 \mathrm{ERB}(f_{r1})/n_1. \quad (5)$$

When fitting the gammachirp filter to human masking data, Irino and Patterson (1997) varied the asymmetry parameter linearly with the probe level of the signal, P_s, measured in dB. In a typical case $c_1 = 3.38 - 0.107 P_s$; c_1 is negative when P_s is greater than about 30 (dB SPL).

B. Filter shape of the analytic gammachirp

In this subsection, we investigate the frequency response of the analytic gammachirp filter. In most cases, the amplitude factor, a_Γ, has been normalized and considered separately from the discussion of the filter shape. We discuss the background and the effect of the amplitude factor in Appendix A and ignore it by setting $a_\Gamma=1$ in Eq. (3).

Figure 1 illustrates how Irino and Patterson (1997) produced a set of gammachirp filters, $|G_C(f)|$, with varying asymmetry, by multiplying a fixed gammatone filter, $|G_T(f)|$, together with a set of asymmetric functions, $\exp(c_1\theta_1)$. The fixed, gammatone auditory filter (GT) is shown by the solid line in the lower part of the figure. The low-pass asymmetric functions (LP-AF) are shown by the fan of dashed lines that pass through the same origin as the gammatone filter; c_1 was varied from 0 to –2 as level increased. The ordinate for the GT and LP-AF filters is on the right-hand side of Fig. 1. Each of the composite gammachirp filters (GC) is produced by multiplying the fixed GT by the appropriate LP-AF (or by adding the decibel values in the figure). The ordinate for the GC filters is on the left-hand side of Fig. 1. The vertical dotted line shows the fixed center

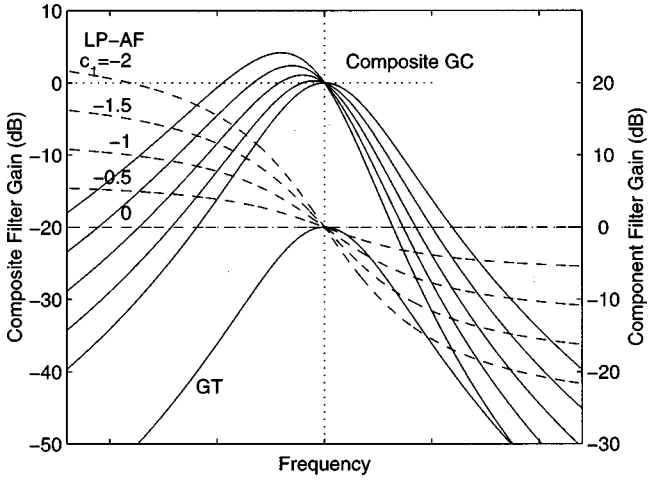

FIG. 1. A set of analytic gammachirp filters, GC (solid lines; left ordinate), produced by cascading a fixed gammatone filter, GT, with a low-pass asymmetric function, LP-AF, whose range varies with level (dashed lines; right ordinate).

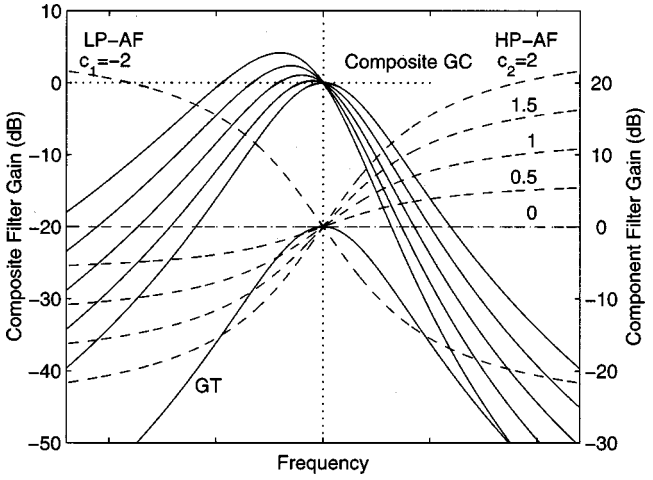

FIG. 2. A set of analytic gammachirp filters, GC (solid lines; left ordinate), produced by cascading a fixed gammatone filter, GT, first with a low-pass asymmetric function, LP-AF (dashed line; right ordinate), and then with a high-pass asymmetric function, HP-AF, whose range increases as level decreases (dashed lines; right ordinate).

frequency of the gammatone auditory filter in the lower part of the figure and the gammachirp with $c_1=0$ in the upper part of the figure; these two filters are, of course, the same. The gain at the peak of this analytic gammachirp filter *increases* with level, as c_1 becomes more negative, and at the same time, the peak frequency of the analytic gammachirp decreases.

There are several problems with the analytic gammachirp filter as a representation of cochlear filtering. The gain at the peak of the filter *increases* with level and the tails of the filters diverge below the center frequency rather than converging. Observations of basilar membrane motion show that as level increases peak frequency decreases as in the analytic gammachirp, but gain *decreases* (Pickles, 1988). Moreover, since the chirp parameter, c_1, is level dependent as described in Irino and Patterson (1997), the trajectory of the chirp changes with level as suggested by Eq. (2). Carney *et al.* (1999) have shown that, although there is a chirp in the impulse response of the cat's cochlear filter, *the form of the chirp does not vary with level* as it does in the analytic gammachirp.

In the next subsections, we describe how the analytic gammachirp filter can be modified to produce a gammachirp filter which is more representative of cochlear observations, and which can explain both the human masking data of Rosen and Baker (1994) and the revcor data of Carney *et al.* (1999).

C. Adapting the architecture of the gammachirp filter to accommodate cochlear observations

Since the chirp does not vary with level it is probably a property of the passive basilar membrane observed at high stimulus levels and post mortem (Recio *et al.*, 1998). The highest-level gammachirp in Fig. 1 has a c_1 of -2, and a brief study revealed that the frequency glide of this gammachirp filter was similar to that observed by Carney *et al.* (1999). This led Irino and Unoki (1999) to reverse the logic of the gammachirp when applying it to the physiology of the cochlea. Instead of simulating the auditory filter with a symmetric gamma*tone* filter at low levels that becomes an asymmetric gammachirp as level increases (for unspecified reasons), they suggested simulating the high-level, passive basilar membrane filter with a fixed, asymmetric, gammachirp filter, which then becomes progressively more symmetric as level decreases by virtue of the active mechanism in the cochlea. They noted that the product of any pair of asymmetric functions is another asymmetric function of the same general form. When an arbitrary value, c_a, is used to define an analytic gammachirp filter, it can be rewritten as follows:

$$\begin{aligned}|G_{CAa}(f)| &= |G_T(f)|\cdot\exp(c_a\,\theta_1)\\ &= |G_T(f)|\cdot\exp(c_1\,\theta_1)\cdot\exp\{(c_a-c_1)\,\theta_1\}\\ &= |G_T(f)|\cdot\exp(c_1\,\theta_1)\cdot\exp(c_2\,\theta_1)\\ &= |G_{CA}(f)|\cdot\exp(c_2\,\theta_1),\end{aligned}\tag{6}$$

where $c_2=c_a-c_1$. $|G_{CA}(f)|$ is an analytic gammachirp filter tied specifically to c_1 as in Eq. (3). Equation (6) shows that a gammachirp filter with an arbitrary shape can be derived from the combination of an initial gammachirp filter with parameter c_1 and an asymmetric function with a carefully chosen c_2. This led them to generate the level-dependent set of gammachirp filters shown in Fig. 2. Each of the composite responses shown by solid lines in the upper part of the figure is the product of (1) a fixed gammachirp filter produced by cascading the gammatone filter (GT) in the lower part of the figure with the fixed, low-pass asymmetric function (LP-AF) having $c_1=-2$, and (2) a second asymmetric function whose c_2 varies between 0 and $+2$, becoming more *positive* as level *decreases*. The result, of course, is the same set of composite gammachirp filters as in Fig. 1. This form of analytic gammachirp filter does not solve the problem of representing cochlear filtering with a family of gammachirp functions; the chirp in the impulse response still varies with level and gain still increases with level. But now the change with level is associated with a high-pass asym-

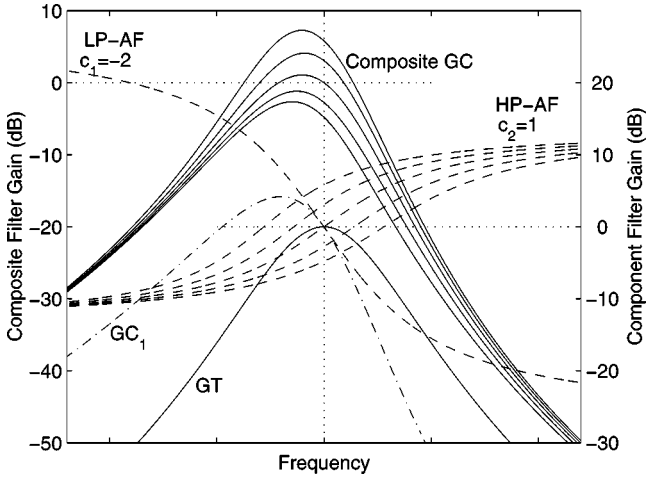

FIG. 3. A set of gammachirp filters, GC (solid lines; left ordinate), produced by cascading a fixed gammatone filter, GT, first with a low-pass asymmetric function, LP-AF (dashed line; right ordinate), and then with a high-pass asymmetric function, HP-AF, whose center frequency, f_{r2}, increases with level (dashed lines; right ordinate). A fixed gammachirp filter, GC_1 (dashed and dotted line; right ordinate) is produced by GT and LP-AF.

metric function (HP-AF) whose effect increases as level decreases, and this form of gammachirp can be developed into a form that is more representative of cochlear physiology.

D. A compressive gammachirp auditory filter

The next step in the process is to rewrite the angular variables of the asymmetric functions in terms of physiological variables and parameters that vary with level, which will then make it possible to fix the values of the asymmetry parameters, c_1 and c_2, so that the chirp does not vary with level. Starting with the form of Eq. (6) in which the representation of both asymmetric functions is explicit,

$$|G_{CC}(f)| = |G_T(f)| \cdot \exp(c_1\,\theta_1) \cdot \exp(c_2\,\theta_2) = |G_{CA}(f)| \cdot \exp(c_2\,\theta_2), \tag{7}$$

the angular variables are rewritten in terms of the center frequencies and bandwidths of the passive gammachirp filter and the level-dependent asymmetric functions. If the filter center frequencies are f_{r1} and f_{r2}, respectively, then from Eq. (4)

$$\theta_1 = \arctan\left(\frac{f - f_{r1}}{b_1 \mathrm{ERB}(f_{r1})}\right) \quad \text{and} \quad \theta_2 = \arctan\left(\frac{f - f_{r2}}{b_2 \mathrm{ERB}(f_{r2})}\right). \tag{8}$$

In this form, the chirp parameters, c_1 and c_2, can be fixed with, for example, $c_1 = -2$, and $c_2 = 1$, and the level dependency can be associated with the center frequency of the *high-pass* asymmetric function, f_{r2}. The center frequency of the low-pass asymmetric function, f_{r1}, is fixed, so that the best frequency of the gammachirp that represents the passive basilar membrane is fixed. If then, for simplicity, $b_2 = b_1$, a new gammachirp filter system is defined with component asymmetric functions and composite gammachirp filters as shown in Fig. 3 by the dashed and solid lines, respectively.[1]

The fixed analytic gammachirp, $|G_{CA}(f)|$, is intended to represent the passive basilar membrane response which is not level dependent; it is presented by the dashed and dotted line in the lower part of the figure (GC_1). This filter largely determines the form of the chirp, and, so, the chirp no longer varies significantly with level. The asymmetric function, $\exp(c_2\,\theta_2)$, of the compressive gammachirp is similar to that of the analytic gammachirp inasmuch as it has a high-pass characteristic that changes with level and renders the composite gammachirp *more symmetric at lower levels*. However, in order to simulate the linearity, or lack of compression, observed in the cochlea at frequencies remote from the best frequency, the asymmetric functions are made to be flat spectrum at frequencies outside the passband. The change with level in the composite gammachirp is achieved primarily by varying the center frequency of the asymmetric function relative to the best frequency of the fixed gammachirp that represents the basilar membrane response. The high-pass asymmetric functions (HP-AF) are shown by the fan of dashed lines in Fig. 3; the function moves up in frequency as level increases. Each of the composite, compressive gammachirp filters is produced by multiplying the fixed GC_1 by the appropriate HP-AF (or by adding the decibel values in the figure). The frequency ratio between the peak frequency f_{p1} in Eq. (5) and the center frequency f_{r2} of the high-pass asymmetric function is

$$f_{\mathrm{rat}} = f_{r2}/f_{p1}. \tag{9}$$

Now, the gain of the composite gammachirp increases and its bandwidth decreases as the center frequency of the high-pass asymmetric function decreases, which agrees, at least qualitatively, with the physiological data. Moreover, the best frequency of the composite filter still shifts down in frequency as level increases, albeit by a relatively small amount in this example. Perhaps most importantly, the chirp no longer varies with level as required by the revcor data of Carney *et al.* (1999). Since this form of the gammachirp filter is compressive around the peak frequency, it is referred to as a compressive gammachirp auditory filter.

The high-pass asymmetric function, $\exp(c_2\,\theta_2)$, does not have an analytic impulse response. An asymmetric compensation filter is developed in Appendix B to enable the simulation of the compressive gammachirp impulse response, so that

$$g_{cc}(t) = a_c \cdot g_{ca}(t) * h_c(t), \tag{10}$$

where a_c is a constant, $g_{ca}(t)$ is the gammachirp impulse response from Eq. (1), and $h_c(t)$ is the impulse response of the asymmetric compensation filter [Appendix B, Eqs. (B4)–(B8)].

III. FITTING THE COMPRESSIVE GAMMACHIRP FILTER TO REVCOR DATA

We characterize the level dependency of the revcor data (Carney *et al.*, 1999) by the level dependency of the parameters of the real function used to represent the auditory filters; that is, the gammatone, the analytic gammachirp, and the compressive gammachirp. We then compare these three filters in terms of the rms fit to physiological data, the number of coefficients in the filter, and the characteristics of the chirp.

A. Parameters

For the analytic gammachirp, the parameters in the fit are, b_1, c_1, f_{r1}, and ϕ_1 in Eq. (1) and the delay of the zero point, τ, which represents the delay of the traveling wave in the cochlea. In the case of the gammatone, the chirp parameter c_1 is set to zero. The compressive gammachirp has eight parameters: b_1, c_1, f_{r1}, ϕ_1, τ, b_2, c_2, and f_{rat}. The amplitude factors a and a_c were not used since both the revcor data and the filter response are normalized. In addition, the order of the gamma distribution, n_1, was fixed to 4 as results of a preliminary simulation and previous studies of the gammatone (de Boer and de Jongh, 1978; Carney and Yin, 1988) and gammachirp (Irino and Patterson, 1997) indicated that this was the appropriate value. The level dependency was introduced as a linear function of noise level, N_r (dB), in the experiment. For example, if the level dependency is applied to the parameter b_1, the formula is

$$b_1 = b_1^{(0)} + b_1^{(1)}(N_r - 80) = b_1^{(0)} + b_1^{(1)} N_{rd}. \tag{11}$$

For convenience in the fitting procedure, we introduced a noise-level parameter, N_{rd}, and we set the coefficient $b_1^{(0)}$ to the value when $N_{rd} = 80$ (dB), which is the common signal level measured for all units. The selection of the level-dependent parameters is described in the following sections.

B. Fitting procedure

The root-mean-squared difference between the revcor data and the filter response was minimized using the Levenberg–Marquardt method (Press *et al.*, 1988). Both the data and the filter were normalized in advance since the gain of the revcor functions varied little with signal level (Carney *et al.*, 1999; Patuzzi and Robertson, 1988). Carney and Yin (1988) measured revcor functions in auditory nerve fibers (or units) over a range of noise levels that depended on how long they held the unit. With one unit they managed ten noise levels (Carney *et al.*, 1999), but with most units it was far fewer. The number of coefficients for the gammachirp filter varies from as few as four up to about ten, and as a result, the coefficients for many units would be theoretically underdetermined. It is also difficult to specify good starting values for the parameters in the sense of producing rapid convergence on a stable solution. Consequently, several techniques were introduced to overcome these problems. First, the fits were performed in two stages; initially, the more stable envelope was fitted to get starting values for the envelope parameters, and then the full impulse response with the fine structure was fitted. Second, for each of these stages, the data at the highest level, 80 dB SPL, was fitted first to determine the zeroth-order coefficients (e.g., $b_1^{(0)}$). Then, with these as starting values, all of the data were fitted to determine all of the coefficients, simultaneously. Finally, we divided the time range of the rms calculation for a given response into two parts—before and after the envelope peak. The number of rms differences is thereby doubled and this is known to assist convergence in least-squared-error methods.

1. Envelope fit

The envelope of the revcor data was calculated over a 20-ms duration as the absolute value of the complex response derived with the Hilbert transform. At the extremes of the interval, where the basilar membrane response was virtually nonexistent, the root-mean-squared (rms) value of the noise was calculated from the revcor data, between 0 and 1 ms and between 18 and 20 ms. An envelope threshold was set at 1.5 times this rms noise level. Envelope values above this threshold were used for calculation of the rms difference. For the analytic gammachirp and the gammatone, the parameters b_1 and τ were included in the least-mean-square process because it is they that mainly determine the envelope shape and the temporal location. For the compressive gammachirp, all parameters except for ϕ_1 were included because they all affect the envelope. Initially, the revcor data for 80 dB SPL were fitted to determine the zeroth-order coefficients $b_1^{(0)}$ and $\tau^{(0)}$. They were then used as the initial values in the next step. The revcor data for all signal levels including 80 dB were used to determine the first-order coefficients $b_1^{(1)}$ and $\tau^{(1)}$ as well as the zeroth-order coefficients $b_1^{(0)}$ and $\tau^{(0)}$. This stage determines the shape of the envelope and its location on the time axis.

2. Waveform fit

Once the envelope was determined with the above procedure, the rest of parameters, f_{r1}, c_1, and ϕ_1 were used to minimize the error between the raw revcor data and the real part of the impulse response for the analytic gammachirp. For the compressive gammachirp, all parameters other than the delay τ are used at this stage. The rms difference between the data and the filter response was calculated within the range where the envelope of the gammachirp is greater than 2% of the peak value. This threshold was established in a preliminary simulation as a tradeoff between maximization of the response length used in the fit and minimization of the background noise in low-power parts of the revcor data. The rms error was defined as the difference between the revcor waveform and the real part of the filter response. The final value was normalized by the rms amplitude of the revcor waveform and specified in dB. As before, the fitting was performed first at 80 dB SPL and then for all signal levels simultaneously.

C. Results: Tradeoffs between accuracy and number of coefficients

This section describes the relationship between the number of coefficients assigned to each parameter and the degree of the fit. The revcor data for Unit 86100u25 with a best frequency of about 2000 Hz was selected from the examples in Fig. 1 of Carney *et al.* (1999) because this unit was measured at ten signal levels which was more than for any other unit. We excluded the data at the lowest level, 20-dB data, because of the relatively high noise level.

1. Fitting with the gammatone filter

First, the revcor data of unit86100u25 was fitted with the real impulse response of the gammatone filter [i.e., $c_1 = 0$ in

TABLE I. Relationship between the number of coefficients and root-mean-square (rms) error for gammatone filters fitted to revcor functions from a cat auditory nerve as reported in Fig. 1(E) (Unit 86100u25, BF=2000 Hz) of Carney *et al.* (1999). The first column shows the total number of coefficients. The second to fifth columns show the number of coefficients used for the gammatone parameter at the top of that column: 1 indicates a filter parameter that is constant across noise level and 2 indicates a linear dependence of the parameter on signal level. The last column shows rms error in dB. The row with the asterisk* shows the parameter set used for Fig. 4.

No. of coefficients	f_{r1}	b_1	ϕ_1	τ	Error
8	2	2	2	2	−10.1
7*	2	2	2	1	−10.1
7	1	2	2	2	−9.8
7	2	2	1	2	−10.0
7	2	1	2	2	−7.3
6	1	2	2	1	−9.9
6	1	2	1	2	−9.8
5	1	2	1	1	−9.8
4	1	1	1	1	−7.6

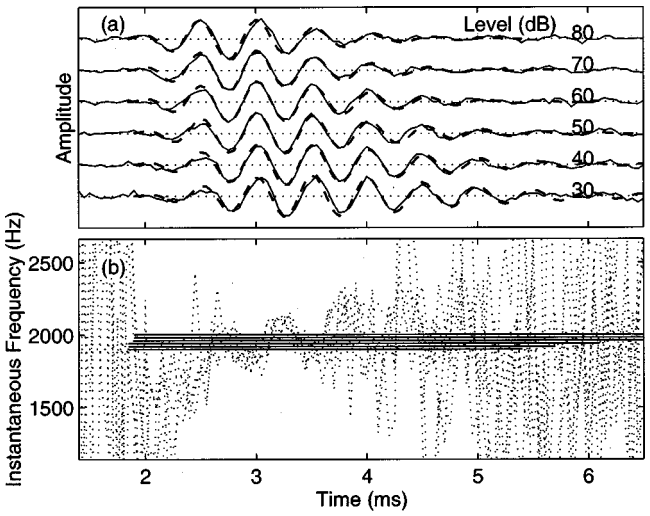

FIG. 4. (a) Normalized revcor functions from unit 86100u25 (solid lines) and the filter responses (dashed lines) of the best-fitting gammatone filter with the parameter set indicated by the asterisk (*) in Table I. The amplitude of the response was normalized by the input signal level indicated by the number on the right-hand side. (b) Instantaneous frequency estimated from the best-fitting gammatone filter (solid lines) and from the revcor functions (dotted lines) using a Hilbert transform after smoothing with a three-point rectangular window.

Eq. (1)]. The parameters for the gammatone are f_{r1}, b_1, ϕ_1, and τ. Table I shows the total number of coefficients (first column), the assignment of coefficients to the parameter (second to fifth columns), and the final rms error in dB between the revcor data and the gammatone filter response (sixth column). The table shows that the gammatone filter can fit the revcor data with an rms error of as little as −10.1 dB when all of the parameters are level dependent. This is a reasonable limit given the noise in the revcor data; the signal-to-noise ratio is less than about 20 dB because the rms noise level is about 10% of the maximum value in the revcor data. At the same time, it is clear that an rms error close to the limit can be achieved with far fewer parameters, so long as the envelope parameter b_1 is level dependent. When b_1 is not level dependent as shown in rows with a 1 in column two, the error increases to between −7.3 and −7.6 dB, which is more than 2 dB worse than the best fit. The reason is illustrated in Fig. 4(a) which presents the revcor impulse responses with solid lines; as signal level increases, the duration of the response decreases and the envelope becomes shorter. The zero-crossings of the carrier are, however, virtually invariant as Carney *et al.* (1999) pointed out. So, it is basically the envelope that is level dependent in these revcor data and b_1 is the main envelope parameter in the gammatone filter.

The impulse responses of the gammatone filters are also plotted in Fig. 4(a) with dashed lines; the case where f_{r1}, b_1, and τ are level dependent is indicated by the asterisk in Table I. This version was used to illustrate the best fit, or the upper limit available with the gammatone filter, rather than the most efficient in terms of the number of parameters per data point. These solutions are presented primarily for comparison with the gammachirp filters in the next subsections. There is good agreement between the data and these gammatone filter responses except in the initial, raising portion of the response between 2 and 2.5 ms.

The instantaneous frequency (IF) of the response was calculated using the Hilbert transform of the average revcor data, smoothed with a three-point rectangular window to reduce abrupt changes in the estimated value. Figure 4(b) shows the instantaneous frequencies estimated for the six levels shown in Fig. 4(a) (dotted lines). The accuracy of the instantaneous frequency data improves rapidly over the first 2 ms and the functions for different levels converge between about 2 and 3.5 ms provided the amplitude is not too low. These IF trajectories show that the chirp does not vary much with level as Carney *et al.* (1999) pointed out. The IF trajectories from the fitted gammatone filters are presented by the solid *straight* lines, and they make it clear that it is impossible to simulate the chirp in the data with the gammatone because the IF of the gammatone is constant, by definition. The main disparities in Fig. 4(b) are observed over the initial portion of the response, and they illustrate that there is a serious limitation in the ability of the gammatone filter to explain revcor data.

2. Fitting with the analytic gammachirp filter

The analytic gammachirp filter of Eq. (1) was used for the fit to the same revcor data of unit86100u25 with five parameters, f_{r1}, b_1, c_1, ϕ_1, and τ. The strategy was the same as described above for the gammatone filter. Table II shows the results. The rms error is reduced to about −11 dB provided the envelope parameter, b_1, is level dependent as indicated by a ''2'' in column three. The fit is improved over that of the gammatone filter by about 1 dB even when the filter has the same number of variable coefficients (e.g., 5 or 6). Making the other parameters level dependent had little effect on the rms error. For example, a comparison between the twelfth and sixteenth rows shows that the delay parameter, τ, does not need to be level dependent. Moreover, the phase parameter, ϕ_1, can be set to zero with little increment in the error term because the initial phase also occurs in the chirp parameter, c_1.[2] In contrast, when the envelope param-

TABLE II. Relationship between the number of coefficients and the rms error for the best-fitting analytic gammachirp filter to the same revcor functions as in Table I. 0 indicates ϕ_1 value of 0. See the caption of Table I for details.

No. of coefficients	f_{r1}	b_1	c_1	ϕ_1	τ	Error
10	2	2	2	2	2	−11.1
9	1	2	2	2	2	−11.0
9	2	2	2	2	1	−11.2
9	2	2	2	1	2	−11.1
9	2	2	1	2	2	−11.2
9	2	1	2	2	2	−7.7
8*	1	2	2	2	1	−11.0
8	1	2	2	1	2	−11.0
8	1	2	1	2	2	−11.0
8	1	1	2	2	2	−7.6
7	1	2	2	1	1	−11.0
7	1	2	1	1	2	−11.0
7	1	2	1	2	1	−11.0
7	1	1	2	2	1	−8.1
7	1	1	2	1	2	−7.7
6	1	2	1	1	1	−11.0
6	1	1	2	1	1	−8.3
5	1	2	1	0	1	−10.7
5	1	1	1	1	1	−8.1

eter, b_1, is not level dependent (rows with a 1 in column three), the rms error increases by around 3 dB to about −8 dB. The reason is the same as for the gammatone filter; the duration of the impulse response decreases with increasing level.

The real parts of the impulse responses of the analytic gammachirp filters are shown with dashed lines in Fig. 5(a); in this version there are eight coefficients as indicated in the row with the asterisk in Table II. This version was selected to fit this unit and other units described in Sec. III D. There is an improvement in the fit, primarily in the first few milliseconds, which reduces the rms error by about 1 dB. The effect is more obvious in Fig. 5(b) which shows the IF trajectories

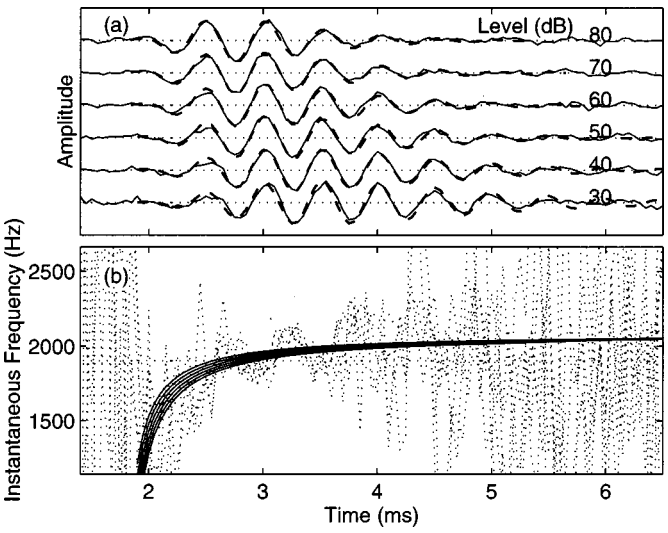

FIG. 5. (a) The same revcor functions as Fig. 4 (solid lines) with responses of the analytic gammachirp filter (dashed lines) using the parameter set indicated by the asterisk (*) in Table II. (b) Instantaneous frequency estimated from the best-fitting analytic gammachirp filter (solid lines) and from the same revcor functions (dotted lines).

TABLE III. Relationship between the number of coefficients and the rms error for the best-fitting compressive gammachirp filter to the same revcor functions as in Table I. The last column shows the average compression between the input and output signal levels in dB/dB. See the captions of Tables I and II for details.

No.	f_{r1}	b_1	c_1	ϕ_1	τ	f_{rat}	b_2	c_2	Error	cmp
10	2	1	1	1	1	2	1	1	−12.0	0.65
10	2	1	1	0	1	2	2	1	−10.0	0.92
9*	2	1	1	0	1	2	1	1	−12.0	0.65
9	1	1	1	1	1	2	1	1	−11.8	0.67
9	1	1	1	0	1	2	2	1	−11.5	0.74
9	2	1	1	1	1	1	1	1	−7.7	1.00
8	1	1	1	0	1	2	1	1	−12.0	0.63
8	2	1	1	0	1	1	1	1	−7.7	1.00

for the analytic gammachirp filters with solid lines [see also Eq. (2)]; they rise smoothly with the average of the revcor data over the duration of the response which is clear of background noise. Thus, the analytic gammachirp provides a good explanation of the revcor data. This analytic gammachirp fit is, however, somewhat different from the one applied by Irino and Patterson (1997) to human masking data; in that case, the chirp parameter, c_1, was level dependent and the envelope parameter, b_1, was not level dependent. This disparity in the level-dependent parameters is one shortcoming of the analytic gammachirp as a model for both physiological and psychophysical data.[3]

3. Fitting with the compressive gammachirp filter

The compressive gammachirp filter of Eq. (10) was used to fit the same revcor data of unit86100u25 with eight parameters, f_{r1}, b_1, c_1, ϕ_1, τ, f_{rat}, b_2, and c_2. In this case, we restricted the maximum number of parameters to ten because the fit would be mathematically underdetermined with nine sets of revcor data. Moreover, ten parameters is sufficient to survey the upper limit of the fitting process. Table III shows the results in the same format as previously: the total number of coefficients (first column), the assignment to parameter (second to ninth columns), and the rms error in dB (tenth column). There is also an extra column showing the average compression in dB/dB (11th column) which will be described shortly. The minimum rms error was −12.0 dB which is better than with the analytic gammachirp by about 1 dB and better than with the gammatone by about 2 dB. When the frequency ratio, f_{rat}, in Eq. (9) is not level dependent (the sixth and eighth rows), the rms error increases about 4 dB to −7.7 dB. So, the relative position in frequency of the initial gammachirp and the high-pass compensation filter needs to be level dependent. Making the other parameters level dependent had little effect on rms error. It also proved possible to set the phase parameter, ϕ_1, to zero without increasing the rms error. The value of the delay parameter, τ, is about 1.8 ms, which is the same as for the analytic gammachirp.

The real parts of the impulse responses of the compressive gammachirp filters are shown with dashed lines in Fig. 6(a); in this version there are nine coefficients as indicated by the asterisk in Table III. Disparities between the revcor data and the filter responses are now limited to the initial and final

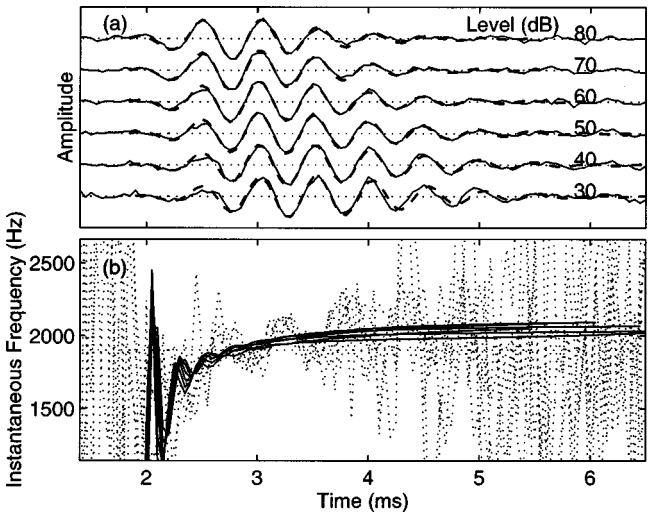

FIG. 6. (a) The same revcor functions as in Fig. 4 (solid lines) with responses of the best-fitting compressive gammachirp filter (dashed lines) using the parameter set indicated by the asterisk (*) in Table III. (b) Instantaneous frequency estimated from the compressive gammachirp filter (solid lines) and from the same revcor functions (dotted lines).

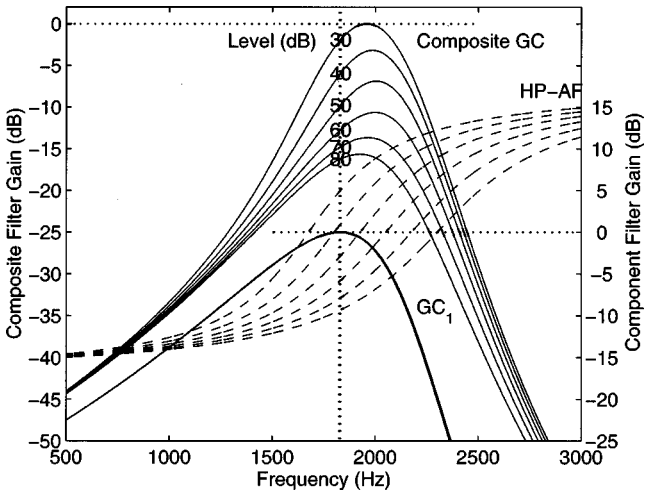

FIG. 7. The set of compressive gammachirp filters, GC (solid lines; left ordinate) derived from the normalized revcor data of Unit 86100u25, corresponding to the impulse responses in Fig. 6(a). The filters were produced by cascading a passive gammachirp filter, GC_1 (lower solid line; right ordinate) with a high-pass asymmetric function, HP-AF (dashed lines; right ordinate) whose center frequency varies with level.

parts of the responses at 30 and 40 dB; the data and filters are almost coincident when the relative amplitude of the waveform is sufficiently large. The level dependence of the frequency ratio, f_{rat}, introduces a level-dependent envelope as described shortly. The IF trajectories of the compressive gammachirp filters are plotted with solid lines in Fig. 6(b). They start with an oscillation and rise with the average of the revcor data. They contrast with the smooth IF trajectories for the analytic gammachirp filters in Fig. 5(b) and Eq. (2). The oscillation is produced by the interaction between the initial, analytic gammachirp filter and the high-pass asymmetric compensation filter. The rapid oscillation seems to contribute to the improvement in the fit, although it is difficult to analyze the effect in detail because the onsets of the revcor functions are at, or below, the noise level.

Figure 7 shows the frequency responses (Composite GC) of the compressive gammachirp filters shown in Fig. 6(a). Each is the composite response of the initial, analytic gammachirp filter (GC_1) and a high-pass asymmetric function (HP-AF). The initial, analytic gammachirp is essentially independent of noise level. The frequency ratio, f_{rat}, is the dominant, level-dependent parameter and it is positively correlated with the noise level. The gain of the auditory filter varies within the passband and it is roughly constant outside the passband. As signal level increases, the peak gain decreases and the bandwidth generally increases. As a result, the envelope in the waveform becomes shorter as the frequency ratio, f_{rat}, becomes larger, since the envelope duration is negatively correlated with bandwidth, provided the carrier frequency does not fluctuate too much.

The peak frequency increases with noise level at first and then it decreases a little. This differs from the typical physiological observation that peak frequency decreases monotonically as level increases. The discrepancy is probably due to a lack of sensitivity to the frequency parameter, f_{r1}, in the current fitting procedure. The fits were restricted to time domain. It is possible that estimation of the change in peak frequency could be improved by introducing constraints from the frequency responses of the revcor data.

The filter gain of the compressive gammachirp varies with noise level. The gain was normalized to 0 dB for a noise level of 30 dB SPL. The gain decreases as noise level increases and is about −16 dB when noise level is 80 dB SPL. Thus, the input–output function of this filter is compressive and the average growth ratio between 30 and 70 dB is about 0.65 dB/dB (see the last column in Table III, labeled ''cmp,'' for an alternative set of coefficients). The compressive gain only occurs in the region of the peak frequency of the filter; the degree of compression decreases and the tails of the filters converge as frequency diverges from the peak frequency. Such compressive gain has been repeatedly reported both physiologically (e.g., Pickles, 1988; Ruggero, 1992) and psychophysically (Oxenham and Plack, 1997). It is not possible to obtain this kind of compression either by varying the amplitude parameter, a, of the analytic gammachirp [Eq. (1)] or the amplitude parameter, a_c, of the compressive gammachirp [Eq. (10)]. It is necessary to invoke a mechanism which affects the amplitude only around the peak frequency. This is accomplished by the interaction of the two component filters in the compressive gammachirp filter.

In summary, the compressive gammachirp filter provides the best account of the revcor data of the three models in terms of rms error, IF trajectory, and compressive gain.

D. Results: Individual units

The frequency glides derived from several units in the same cat (86100) were reported in Fig. 4 of Carney *et al.* (1999). The instantaneous frequencies were determined directly using the zero crossings of the revcor waveforms without any parametric model. First-order regression lines were plotted on the same figure to show the general trends. We have characterized the IF trajectory with parametric models, namely, the analytic gammachirp and the compressive gam-

TABLE IV. Parameter values and rms errors for the best-fitting analytic gammachirp filters to the revcor functions from various units of cat 86100 (see Fig. 4 of Carney *et al.*, 1999). The first column shows the unit number. The second column shows the number of sound pressure levels measured for the unit. The last column shows rms error in dB. The remaining columns show the best-fitting coefficients for f_{r1}, b_1, c_1, ϕ_1 τ when $n_1=4$, $N_{rd}=N_r-80$.

Unit	Level no.	f_{r1}	b_1	c_1	ϕ_1	τ	Error
20	2	303	$2.39+0.010N_{rd}$	$1.18-0.001N_{rd}$	$0.96-0.000N_{rd}$	2.10	−10.0
2	2	463	$2.57+0.015N_{rd}$	$1.29+0.017N_{rd}$	$1.92+0.113N_{rd}$	2.10	−10.7
22	4	1150	$2.66+0.022N_{rd}$	$0.11+0.012N_{rd}$	$1.18+0.102N_{rd}$	2.46	−10.3
7	5	1660	$1.82+0.013N_{rd}$	$-0.60+0.002N_{rd}$	$-1.17+0.022N_{rd}$	1.78	−12.7
25	9	2085	$1.89+0.016N_{rd}$	$-1.39-0.009N_{rd}$	$-0.41-0.054N_{rd}$	1.73	−11.0
26	6	2676	$1.54+0.013N_{rd}$	$-2.54+0.022N_{rd}$	$2.05+0.123N_{rd}$	1.50	−10.2
18	2	3100	$1.38+0.021N_{rd}$	$-2.86+0.017N_{rd}$	$-2.59+0.389N_{rd}$	1.42	−8.5

machirp. In this section we describe the fitting of these IF models to the revcor data presented by Carney *et al.* (1999) in their Fig. 4 (units 2, 7, 18, 20, 22, and 26).

1. Parameter values

We used the analytic gammachirp with eight coefficients and the compressive gammachirp with nine coefficients as indicated by asterisks in Tables II and III, respectively. They both have more than the minimum number of coefficients required to fit one of the units (25), but it seemed desirable to use the same parameter set for all units. It is also the case that the revcor functions for several units (units 2, 18, and 20) were only measured at two signal levels. Fairly substantial preliminary simulation was used to select initial coefficients for each unit to get reasonable convergence. The simulations were then repeated with one additional coefficient (nine for the analytic gammachirp; ten for the compressive gammachirp) to confirm that the results are stable.

The values of coefficients associated with the fits that produced the minimum rms error are listed in Table IV for the analytic gammachirp and in Table V for the compressive gammachirp. The first column shows the unit number; the second column shows the number of noise levels used in the fit; and the column labeled error shows the rms error in dB. The extra column labeled ''cmp'' in Table V shows the compression factor in dB/dB. The remaining columns show the parameter values as before. The average rms error for the analytic and compressive gammachirp are −10.5 dB and −10.4 dB, respectively. So, the quality of the fits is about the same. The problem is that there are not really sufficient noise levels for units other than 25.

For the analytic gammachirp (Table IV), the parameters b_1, c_1, and ϕ_1 are level dependent. Both the envelope parameter, b_1, and chirp parameter, c_1, are negatively correlated with the frequency, f_{r1}, when noise level N_{rd} is constant; the phase parameter, ϕ_1, does not show a clear tendency. It is difficult to imagine a physical realization of this phase term in a cochlear simulation where the parameter is gradually changing with location. For the compressive gammachirp (Table V), only the frequency parameters, f_{r1} and f_{rat}, are level dependent. The phase parameter, ϕ_1, is zero. All of the other parameters are level independent. The delay parameter, τ, is level independent in both filter models and the values are virtually the same for corresponding units in Tables IV and V. The values are about 2 ms when the frequency parameter, f_{r1}, is below 1000 Hz; they are less than 2 ms and negatively correlated to best frequency when f_{r1} is above 1000 Hz.

The average compression of the input-output function is about 0.65 dB/dB when the revcor data span six to nine noise levels and about 0.8 dB/dB when the revcor data span four to five noise levels. No consistent value is obtained for units with only two noise levels. The best estimate of the compression value is obtained from revcor data measured for a wide dynamic range, and a relatively large number, of noise levels. So, a value of about 0.6 dB/dB in the frequency region of 2 kHz seems a reasonable overall summary of the current results with regard to compression. This value is in good agreement with values derived from physiological observations of input-output functions in auditory nerve fibers of guinea-pig with similar CFs (Cooper and Yates, 1994). They are also in good agreement with recent psychophysical mea-

TABLE V. Parameter values, rms errors, and degree of compression for the best-fitting compressive gammachirp filters to the same revcor functions as in Table IV. The last column shows the compression ratio between the input and output of the filter in dB/dB. Columns 3–10 show the best-fitting coefficients when $n_1=4$. See the caption of Table IV for further details.

Unit	No.	f_{r1}	b_1	c_1	ϕ_1	τ	f_{rat}	b_2	c_2	Error	cmp
20	2	$290+0.094N_{rd}$	2.67	−1.15	0	2.10	$1.00+0.0015N_{rd}$	1.96	2.84	−9.5	0.94
2	2	$420+0.004N_{rd}$	1.94	−0.38	0	2.08	$1.21+0.0043N_{rd}$	1.72	2.18	−10.9	0.75
22	4	$1110+2.017N_{rd}$	2.02	−0.63	0	2.33	$1.16+0.0042N_{rd}$	1.51	1.03	−9.8	0.82
7	5	$1600-0.085N_{rd}$	1.62	−1.70	0	1.52	$1.09+0.0030N_{rd}$	0.94	1.30	−10.4	0.81
25	9	$2150-0.144N_{rd}$	1.67	−3.03	0	1.77	$1.26+0.0069N_{rd}$	1.57	1.29	−12.0	0.65
26	6	$2500-0.034N_{rd}$	1.65	−2.92	0	1.66	$1.21+0.0050N_{rd}$	1.38	1.48	−11.2	0.67
18	2	$3100+0.000N_{rd}$	1.36	−3.37	0	1.46	$1.24+0.0168N_{rd}$	1.08	0.99	−8.8	0.25

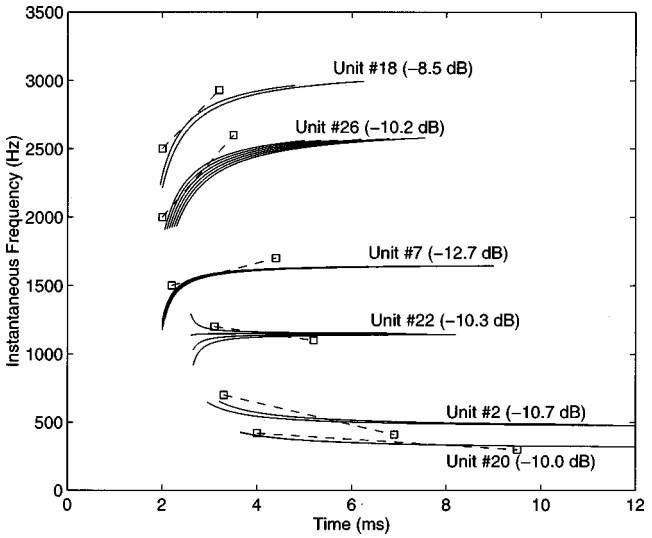

FIG. 8. Instantaneous frequency trajectories for six units from cat 86100. Dashed lines terminated with squares are adapted from the first-order regression lines for 80 dB SPL in Fig. 4 of Carney *et al.* (1999). Solid lines show the instantaneous frequency estimated from the analytic gammachirp filter, for all sound pressure levels. The filter coefficients are shown in Table IV. The unit number and rms error (in parentheses) are shown beside the curves.

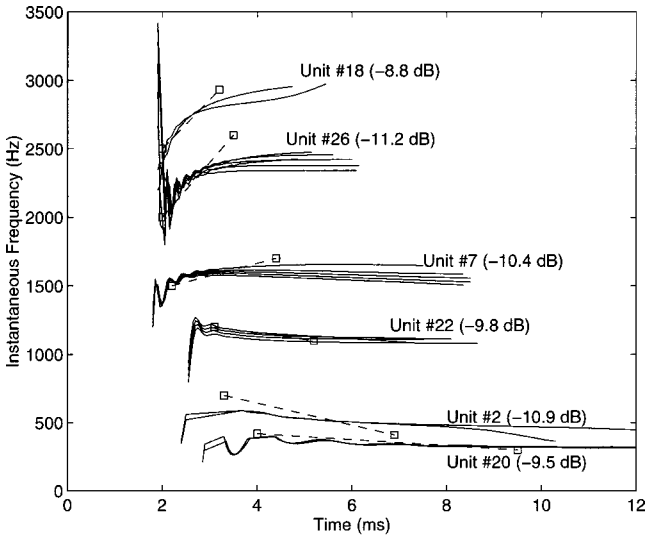

FIG. 9. Instantaneous frequency trajectories for six fibers of cat 86100. Dashed lines show first-order regression lines for 80 dB SPL by Carney *et al.* (1999, Fig. 4). Solid lines show instantaneous frequencies from the best-fitting compressive gammachirp filters. The filter coefficients are shown in Table V. The rms errors are shown in parentheses.

surements of compression derived from forward masking experiments in the frequency region 1500–3000 Hz (Hicks and Bacon, 1999).

2. Instantaneous frequency

The IF trajectories were calculated from the complex responses of the analytic and compressive gammachirp filters using the parameter values listed in Tables IV and V. The dashed lines with squares in Figs. 7 and 8 show the first-order regression lines fitted to the IF values derived at the 80-dB level by Carney *et al.* (1999, Fig. 4) for units, 2, 7, 18, 20, 22, and 26. The solid lines show the IF trajectories within the range where the envelope magnitude is greater than 2% of the envelope peak (the same criterion as was used when calculating the rms error in Sec. II B).

Figure 8 shows that the IF trajectories for the analytic gammachirp flow through the bounds delimited by the regression lines. The IFs for units 7, 26, and 18 glide upward from a very low IF to asymptote in the region of the best frequency of the unit. This is consistent with the results for unit 25 described previously. The IFs for units 2 and 20 glide downward from a very high IF to asymptote in the region of the best frequency of the unit. Theoretically, the downward frequency glide starts at infinity. The IFs for unit 22 glide in to the best frequency either from well below or well above depending on the sign of the chirp parameter, c. For example, the c values are 0.11 and -0.37 for noise levels of 80 and 40 dB, respectively. It is difficult to imagine the mechanism associated with an IF starting from infinite frequency, or one whose starting point flips from infinity to 0 as noise level increases. In summary, the analytic gammachirp provides a reasonable fit to the IF data in terms of rms error, but it does not provide useful insights into the cochlear mechanisms underlying the initial portion of the IF trajectory.

Figure 9 shows that the IF trajectories for the compressive gammachirp also flow through the bounds delimited by the regression lines. The IF trajectories for units 2, 20, and 22 rise rapidly from zero frequency to a maximum value and, then, *decrease* gradually. Since the IFs do not start from infinite frequency, the responses are more realistic in terms of the underlying cochlear mechanics. The trajectories for units 26 and 18 have initial frequencies higher than their asymptotic frequencies and they oscillate on the way to the asymptote. The maxima in these functions arise from low-amplitude parts of the filter response; no corresponding maxima are observable in the revcor data because of the low signal-to-noise ratio. It is, nevertheless, interesting to note that there are oscillations in the original IF data of units 26 and 18 (Fig. 4 of Carney *et al.*, 1999), although they do not have the same period partly due to methodological differences in the IF calculation. In summary, the compressive gammachirp provides a reasonable fit to the IF data in terms of rms error.

IV. FITTING THE COMPRESSIVE GAMMACHIRP TO HUMAN MASKING DATA

Irino and Patterson (1997) demonstrated that the analytic gammachirp filter can explain a wide range of notched-noise masking data. The most demanding data were those of Rosen and Baker (1994) who measured masking over a large dynamic range. In this section, we show how the compressive gammachirp can be fitted to these data, and thereby raise the prospect that the compressive gammachirp filter can provide the basis for a unified model of frequency selectivity in the auditory system.

A. Method and parameters

In the psychophysical experiment, the observer is required to detect a brief probe tone in the presence of a low-pass or high-pass noise masker (Patterson, 1974). As the dis-

placement between the tone frequency and the edge of the noise increases, threshold decreases over a range that can be as much as 60 dB. It is assumed that the observer listens for the tone through an auditory filter centered in the region of the tone to maximize the signal level and minimize the noise level in the decision variable. The slope of the noise cutoff is very steep and the spectrum level of the noise is flat, and in this case, the function relating probe threshold to the frequency of the noise cutoff is closely related to the integral of the auditory filter. This relationship provides the basis for the fitting procedure (Patterson *et al.*, 1982) and the large dynamic range of the threshold measurements means that the procedure can be highly sensitive to filter shape. Over the years, the assumptions of the model have been tested and the procedure has been improved in conjunction with the fitting technique, for example, to ensure that the auditory filter is centered close to the tone frequency and to accommodate filter asymmetry (Patterson and Nimmo-Smith, 1980). Reviews of the development and extension of the technique are provided in Patterson and Moore (1986) and Rosen and Baker (1994). Basically, however, the technique remains the same; probe level at threshold is used in conjunction with carefully designed noise maskers to estimate the integral of the auditory filter, and functions like the gammachirp are then fitted to sets of these thresholds to determine the optimal parameter values to represent the auditory filter.

The compressive gammachirp was fitted to the notched-noise data of Rosen and Baker (1994) using basically the same procedure as in Irino and Patterson (1997).[4] The Levenberg–Marquardt method (Press *et al.*, 1988) was employed to minimize the rms difference between the masked threshold in dB and the predicted value of masked threshold, also in dB. Since the data are now thresholds values, in dB, the value of the rms error is somewhat different from that used to fit to revcor data. It is also worth noting that the rms errors are based on values with different units near the probe frequency, unlike the rms error in the fit to a single unit of revcor data. These factors do not affect the consistency of filter derivation with the revcor data because a single compressive gammachirp filter is used for each parameter set. The probe frequency in the psychophysical experiment was 2000 Hz and the data were gathered for a very wide range of both probe and masker levels.

The compressive gammachirp has essentially nine parameters (n_1, b_1, c_1, f_{r1}, ϕ_1, b_2, c_2, f_{rat}, and τ) as described in Eqs. (1)–(8) of Sec. II. However, the phase parameter, ϕ_1, and the delay parameter, τ, cannot be specified in this case because we use the magnitude spectrum, $|G_{\mathrm{CC}}(f)|$, to fit the masking data. Instead, the procedure requires two other parameters which are the efficiency of the detector, K, that determines the listeners response, and a limit on the dynamic range, r, of the filter. In this case, r was set to -100 dB which is virtually zero. The amplitude parameter a_c falls out of the fitting equations with masking data since both the data and the filter response are normalized. Once again, the order of the gamma distribution, n_1, was fixed at 4.

To control for off-frequency listening (Patterson and Nimmo-Smith, 1980), the asymptotic frequency, f_{r1}, of the analytic gammachirp, $g_{ca}(t)$, and thus its peak frequency, f_{p1}, were varied to locate the filter position that produces the maximum signal-to-noise ratio in each listening condition. The fits to the revcor data (Tables III and V) show that the frequency ratio, f_{rat}, needs to vary with level to produce a good fit, but that the other parameters do not. Accordingly, the frequency ratio, f_{rat}, was set to be a linear function of probe level, P_s, in dB; the remaining parameters (b_1, c_1, b_2, c_2, and K) were taken to be level-independent variables.

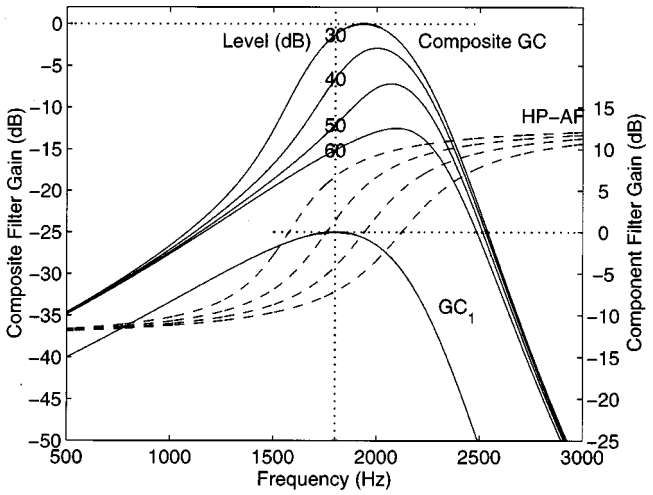

FIG. 10. The set of compressive gammachirp filters, GC (solid lines; left ordinate) derived from Rosen and Baker's data (1994). The filters were produced by cascading a passive gammachirp filter, GC_1 (lower solid line; right ordinate) with a high-pass asymmetric function, HP-AF (dashed lines; right ordinate) whose center frequency varies with level.

B. Results

The best fit resulted in a rms error of 1.27 (dB), which is slightly better than the 1.36 dB produced with by Irino and Patterson (1997) with the original, analytic gammachirp.[5] The parameter values in this case are $b_1=2.02$; $b_2=1.14$; $c_1=-3.70$; $c_2=0.979$; $f_{\mathrm{rat}}=0.573+0.0101P_s=1.381+0.0101\cdot(P_s-80)$; $K=-5.03$. So, it is sufficient to make the ratio of frequencies level dependent to explain the masking data; none of the other parameters need vary with level in this specific case. It is also interesting to note that, although the masking data and the revcor data are completely different, the parameter values for the masking data fall within the range of parameter values listed in Table V for the fit of the compressive gammachirp to revcor data.

The magnitude spectra for the best-fitting filters are shown in Fig. 10 for the case where the peak frequency, f_{p1}, of the fixed, analytic gammachirp (lower solid line) is 1800 Hz (the asymptotic frequency, f_{r1}, is about 2300 Hz). Since the frequency ratio, f_{rat}, is level dependent, the high-pass asymmetric function is level dependent as indicated by the set of dashed curves. Consequently, the composite, compressive gammachirp filter is level dependent as shown by the set of solid lines in the upper portion of the figure. As signal level increases, the peak gain decreases and the bandwidth generally increases (although it is slightly non-monotonic). Here, then, is an auditory filter with level-dependent gain in

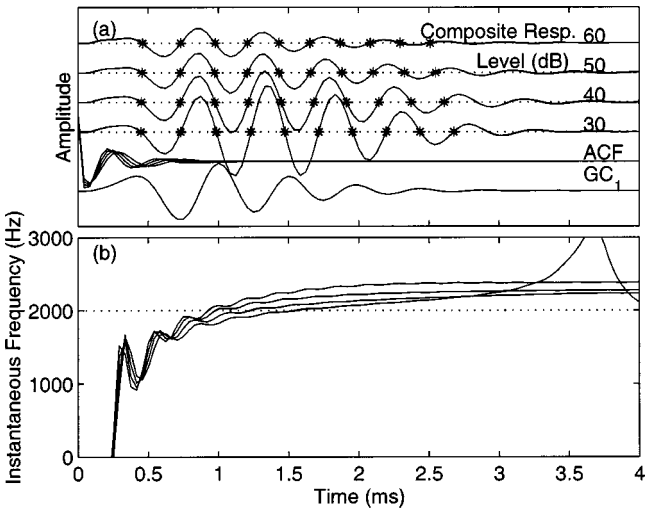

FIG. 11. The impulse response (a) and instantaneous frequency trajectory (b) of the compressive gammachirp filter shown in Fig. 10. In panel (a), the bottom line shows the response of the initial gammachirp filter, GC_1, and just above it the responses of the high-pass, asymmetric compensation filters, ACF. The upper four lines show the responses of the composite compressive gammachirp filters as a function of stimulus level (dB). Since the responses are normalized by the input signal level, the maximum amplitude corresponds to the filter gain. The asterisks show the times of the seven zero-crossings in the responses. In panel (b), the four lines present the instantaneous frequency trajectory for the four composite gammachirp filters in panel (a).

the passband and linear tails outside the passband, as required physiologically, that can accommodate human masking data over a wide dynamic range. In contrast to the physiological observations, the peak frequency increases slightly with level. This is because the peak frequency, f_{p1}, of the analytic gammachirp is assumed to be fixed. The discrepancy with physiological data can be resolved if f_{p1} is made level dependent and negatively correlated with level, as is the case for units 25 and 26 in Table V. It is not possible, however, to determine the relationship between f_{p1} and level with notched-noise data because the fitting procedure includes the assumption that the listeners use ''off-frequency listening'' to optimize signal detection (Patterson and Nimmo-Smith, 1980). That is, the listeners use the filter that gives the maximum signal-to-noise ratio in any given condition and the optimum filter varies with masking condition.

The impulse responses of the filters shown in Fig. 10 are plotted in Fig 11(a). In this case, the unspecified parameters were set to zero (the phase, ϕ_1, and the latency, τ). The filter gain (relative amplitude) decreases as level increases, but the locations of the zero crossings (indicated by asterisks) are almost level independent at least for the first few cycles where the amplitude of the filter is sufficiently high. The filter responses are similar to those from the revcor data shown in Fig. 6(a) except that the gain of the revcor data was normalized. The IF trajectories calculated from the impulse responses in Fig. 11(a) are plotted in Fig. 11(b). The characteristics of the frequency-glide are quite similar to those of the IF trajectories shown in Fig. 6(b). So, the results are consistent with the physiological observations of Carney *et al.* (1999).

The gain of the compressive gammachirp filter decreases as level increases. So, there is compression between the input and output of the filter in the passband. The average compression is about 0.6 dB/dB which is similar to the values obtained with the revcor data of units 25 and 26 in Table V.

V. SUMMARY

The analytic, gammachirp auditory filter of Irino and Patterson (1997) has been extended to produce a new gammachirp auditory filter that can provide a unified framework for both physiological and psychophysical modeling of frequency selectivity and compression. This compressive gammachirp filter consists of an analytic gammachirp with a fixed, negative chirp parameter and a high-pass asymmetric function with a positive chirp parameter. The compressive gammachirp filter provides a better fit to the revcor data of Carney *et al.* (1999), in terms of rms error, than either the gammatone auditory filter or the analytic gammachirp filter. It is also more compatible with observations of basilar membrane motion and primary auditory nerve data which show that the chirp in the impulse response is not level dependent. The compressive gammachirp filter was also fitted to the human masking data of Rosen and Baker (1994) without the level-dependent chirp previously required to fit such data. It appears that both cat revcor data and human masking data can be explained with a single compressive gammachirp filter that has only one level-dependent parameter, which is the ratio of the frequencies that defined the positions of the filter's components—the fixed analytic gammachirp and the high-pass asymmetric function. Thus, the compressive gammachirp filter provides a relatively simple model for characterizing the cochlear frequency glide and predicting human masking data within a unified framework.

ACKNOWLEDGMENTS

We would like to thank L. Carney for providing us with the revcor data and Richard Baker for helpful comments on an earlier draft of the paper. This research was mainly performed when the first author was seconded to, and the second author was a visiting researcher at ATR-HIP, Kyoto. The research was partially supported by CREST (Core Research for Evolutional Science and Technology) of the Japan Science and Technology Corporation (JST) and a grant from ATR-HIP to the second author at the Center for the Neural Basis of Hearing in Cambridge.

APPENDIX A: AMPLITUDE FACTOR OF THE GAMMACHIRP

The Fourier magnitude spectrum of the gammachirp filter in Eq. (1) is

$$|G_C(f)| = \frac{a|\Gamma(n_1+jc_1)|}{|2\pi\sqrt{\{b_1\mathrm{ERB}(f_{r_1})\}^2+(f-f_{r_1})^2}|^n}\cdot \exp(c_1\,\theta_1)$$

$$= \frac{a\,|\Gamma(n_1+jc_1)|}{\Gamma(n_1)} \times \frac{\Gamma(n_1)}{|2\pi\sqrt{\{b_1\mathrm{ERB}(f_{r_1})\}^2+(f-f_{r_1})^2}|^n}\cdot \exp(c_1\,\theta_1)$$

$$= a_\Gamma \cdot |G_T(f)| \cdot \exp(c_1\,\theta_1), \tag{A1}$$

$$\theta_1 = \arctan\left(\frac{f-f_{r_1}}{b_1\mathrm{ERB}(f_{r_1})}\right). \tag{A2}$$

The scalar values a, b_1, c_1, f_{r_1}, and n_1 are the amplitude, bandwidth, chirp factor, asymptotic frequency, and envelope factor of the filter, and $\mathrm{ERB}(f_{r_1})$ is the equivalent rectangular bandwidth. The first term, a_Γ, in Eq. (A1) is the power normalization factor from the definition of the Fourier transform. When the envelope factor, n_1, is an integer,

$$a_\Gamma = \frac{a|\Gamma(n_1+jc_1)|}{\Gamma(n_1)} = \frac{a}{\Gamma(n_1)}\cdot\sqrt{\frac{\pi}{c_1\sinh(\pi c_1)}}\cdot\prod_{k=0}^{n_1-1}|k+jc_1|$$

$$= a\sqrt{\frac{\pi c_1}{\sinh(\pi c_1)}}\cdot\prod_{k=1}^{n_1-1}\left|1+j\frac{c_1}{k}\right|. \tag{A3}$$

The second factor in Eq. (A1), $|G_T(f)|$, is the Fourier magnitude spectrum of the gamma*tone* auditory filter. The third factor, $\exp(c_1\,\theta_1)$, is the asymmetric function which introduces asymmetry into the frequency response and converts it into a gamma*chirp* auditory filter. This is a lowpass filter when $c_1<0$, a highpass filter when $c_1>0$, and unity when $c_1=0$.

The peak gain of the analytic gammachirp filter in Fig. 1 is

$$\frac{|G_C(f_{p1})|}{|G_C(f_{r_1})|} = \frac{\exp\{c_1\cdot\arctan(c_1/n_1)\}}{\{1+(c_1/n_1)^2\}^{n_1/2}}, \tag{A4}$$

where f_{p_1} is the peak frequency defined in Eq. (5).

The peak gain can be normalized to unity (0 dB) using Eq. (A4). It is also possible to normalize the power using a_Γ in Eq. (A3). In this case, the peak gain decreases slightly as the chirp factor, c, decreases (to about -0.5 dB when $c_1=-2$). There is, however, no clear physiological criterion for selecting a particular gain factor.

In the process of fitting the gammachirp to human masking data, Irino and Patterson (1997) attributed any shifts in peak frequency to 'off-frequency listening' (Patterson and Nimmo-Smith, 1980), and any changes in gain were aggregated into the efficiency constant, K, which is described with reference to the roex filter in Patterson *et al.* (1982). So, the peak gain was essentially normalized to unity when fitting the data. As a result, the effects of level on gain and peak frequency, and thus the relationship to physiological data, were not discussed in that paper.

The amplitude factor cannot be derived from the revcor data because the discharge rates of auditory nerve fibers saturate as the noise level increases (Patuzzi and Robertson, 1988; Carney *et al.*, 1999). As a result, both the amplitude of the filter response and the data were normalized in the process of fitting filters to the revcor data. The compressive gammachirp filter has the advantage that the compression characteristics can be determined without the need to specify the amplitude factor, as demonstrated in Fig. 3. It does, however, mean that further experiments will be necessary to determine whether the amplitude factor is level-dependent.

APPENDIX B: ASYMMETRIC COMPENSATION FILTER (ACF) AND ASYMMETRIC FUNCTION

Equation (7) shows that the compressive gammachirp, $G_{CC}(f)$, is defined as the combination of another gammachirp, $G_{CA}(f)$, and an asymmetric function, $\exp(c_2\,\theta_2)$. The impulse response of the gammachirp is described in Eq. (1). The impulse response of the asymmetric function, however, is not well-defined because the phase response is not specified in Eqs. (3) and (7). Recently, while implementing a gammachirp filterbank for auditory modeling, Irino and Unoki (1998, 1999) developed an IIR asymmetric compensation filter, $H_C(f)$, to simulate the asymmetric function such that

$$|H_C(f)| \cong \exp(c\cdot\theta), \tag{B1}$$

$$G_C(f) \cong G_T(f)\cdot H_C(f), \tag{B2}$$

and, for the impulse response,

$$g_c(t) \cong g_t(t) * h_c(t). \tag{B3}$$

The asymmetric compensation filter is defined in the z plane as

$$H_C(z) = \prod_{k=1}^{N} H_{Ck}(z), \tag{B4}$$

$$H_{Ck}(z) = \frac{(1-r_k e^{j\varphi_k} z^{-1})(1-r_k e^{-j\varphi_k} z^{-1})}{(1-r_k e^{j\phi_k} z^{-1})(1-r_k e^{-j\phi_k} z^{-1})}, \tag{B5}$$

$$r_k = \exp\{-k\cdot p_1\cdot 2\pi b\mathrm{ERB}(f_r)/f_s\}, \tag{B6}$$

$$\phi_k = 2\pi\{f_r + p_0^{k-1}\cdot p_2\cdot c\cdot b\mathrm{ERB}(f_r)\}/f_s, \tag{B7}$$

$$\varphi_k = 2\pi\{f_r - p_0^{k-1}\cdot p_2\cdot c\cdot b\mathrm{ERB}(f_r)\}/f_s, \tag{B8}$$

where p_0, p_1, and p_2 are positive coefficients, f_s is the sampling rate, and N is the number of filters in the cascade. When $N=4$, $p_0=2$, and p_1 and p_2 are properly set as a function of $|c|$, the rms error in the Fourier magnitude spectra between the original gammachirp filter, $|G_C(f)|$, and the composite filter, $|G_T(f)|\cdot|H_C(f)|$, is reduced to less than 1 dB within the range required by parameters b and c. The accuracy is greatest near the asymptotic frequency, f_r, and, as a result, the impulse responses are in excellent agreement. [For details, see Irino and Unoki (1998, 1999).]

As a result, the impulse response of the asymmetric compensation filter is used to fit the revcor data in the time domain, and the asymmetric function is used to fit the human masking data in the frequency domain.

[1]The idea of combining an analytic gammachirp with a high-pass asymmetric function was originally inspired by the NonLinear Resonant Tectorial Membrane (NL-RTM) model of Allen (1997, 1998). In this model, two filters interact as a function of level: the first filter has a bandpass characteristic and it represents the basilar membrane (BM) travelling wave; the second filter has more of a highpass characteristic and it represents the interaction between the basilar and tectorial membranes (BM-TM filter). The location of the peak of the BM motion moves relative to the BM-TM filter as a function of signal level. The magnitude of mechanical vibration is plotted as a function of cochlear location, as for an excitation pattern. These excitation patterns can be reinterpreted as the magnitude spectra of auditory filters using the conversion scheme proposed by Glasberg and Moore (1990), and in this case, the filter shape is found to be similar to those in Fig. 3. It still remains, however, to determine whether the conversion is applicable to physiological observations of basilar membrane motion.

[2]It is easy to show that the chirp parameter, c_1, affects the initial phase. When $c_1 \ln t$ in Eq. (1) is expanded to $c_1 \ln t/t_0 + c_1 \ln t_0$, t_0 is a constant, and so $c_1 \ln t_0$ is a phase term.

[3]We fitted gammachirp filters to revcor functions derived with sustained noise and based on the assumption of linearity. It has been reported that when the measurements are made with clicks, the envelope becomes longer as level increases (Lin and Guinan, 2000), which contradicts the linearity assumption. To accommodate such data, it would be essential to introduce a mechanism to estimate the internal level of a transient and a controller to set the appropriate values of the filter parameters for that level. Such a mechanism is beyond the scope of this article.

[4]There are two further differences between the fit of Irino and Patterson (1997) and that used here: a correction for equal loudness contour (ELC) has been included as suggested by Glasberg and Moore (1990), and the fixed absolute threshold value of 22.7 dB was omitted because it was initially introduced by Rosen and Baker (1994) for their specific data and is not applicable to other masking data.

[5]The fit with the original gammachirp (in Fig. 2 of Irino and Patterson, 1997) was recalculated with the conditions in footnote 4; the result was 1.36 dB, which is slightly higher than 1.33 dB originally reported.

Allen, J. B. (**1997**). ''OHCs shift the excitation pattern via BM tension,'' in *Diversity in Auditory Mechanics*, edited by Lewis, E. R., *et al.* (World Scientific, Singapore).

Allen, J. B. (**1998**). ''A bio-mechanical model of the ear to predict auditory masking,'' in Proc. Computational Hearing (NATO Advanced Study Institute), Il Ciocco, Italy.

Carney, L. H. (**1993**). ''A model for the response of low-frequency auditory-nerve fibers in cat,'' J. Acoust. Soc. Am. **93**, 401–417.

Carney, L. H., and Yin, T. C. T. (**1988**). ''Temporal coding of resonances by low-frequency auditory nerve fibers: single-fiber responses and a population model,'' J. Neurophysiol. **60**, 1653–1677.

Carney, L. H., Megean, J. M., and Shekhter, I. (**1999**). ''Frequency glides in the impulse responses of auditory-nerve fibers,'' J. Acoust. Soc. Am. **105**, 2384–2391.

Cooke, M. (**1993**). *Modelling Auditory Processing and Organisation* (Cambridge U. P., Cambridge).

Cooper, N. P., and Yates, G. K. (**1994**). ''Nonlinear input-output functions derived from the responses of guinea-pig cochlear nerve fibres: Variations with characteristic frequency,'' Hear. Res. **78**, 221–234.

de Boer, E. (**1975**). ''Synthetic whole-nerve action potentials for the cat,'' J. Acoust. Soc. Am. **58**, 1030–1045.

de Boer, E., and de Jongh, H. R. (**1978**). ''On cochlear encoding: Potentialities and limitations of the reverse-correlation technique,'' J. Acoust. Soc. Am. **63**, 115–135.

de Boer, E., and Nuttall, A. L. (**1997**). ''The mechanical waveform of the basilar membrane. I. Frequency modulations (glides) in impulse responses and cross-correlation functions,'' J. Acoust. Soc. Am. **101**, 3583–3592.

de Boer, E., and Nuttall, A. L. (**2000**). ''The mechanical waveform of the basilar membrane. III. Intensity effects,'' J. Acoust. Soc. Am. **107**, 1497–1507.

Glasberg, B. R., and Moore, B. C. J. (**1990**). ''Derivation of auditory filter shapes from notched-noise data,'' Hear. Res. **47**, 103–138.

Hicks, L. M., and Bacon, S. P. (**1999**). ''Psychophysical measures of auditory nonlinearities as a function of frequency in individuals with normal hearing,'' J. Acoust. Soc. Am. **105**, 326–338.

Irino, T., and Patterson, R. D. (**1997**). ''A time-domain, level-dependent auditory filter: The gammachirp,'' J. Acoust. Soc. Am. **101**, 412–419.

Irino, T., and Patterson, R. D. (**2000**). ''A gammachirp framework for auditory filtering: Unification of cochlear frequency-glide data and psychoacoustical masking data,'' 12th International Symposium on Hearing, Mierlo, The Netherlands.

Irino, T., and Unoki, M. (**1998**). ''A time-varying, analysis/synthesis auditory filterbank using the gammachirp,'' IEEE Int. Conf. Acoust. Speech Signal Processing (ICASSP-98), Seattle, WA, pp. 3653–3656.

Irino, T., and Unoki, M. (**1999**). ''A analysis/synthesis auditory filterbank based on an IIR implementation of the gammachirp,'' J. Acoust. Soc. Jpn. **20**, 397–406.

Johannesma, P. I. M. (**1972**). ''The pre-response stimulus ensemble of neurons in the cochlear nucleus,'' in *Symposium on Hearing Theory* (IPO, Eindhoven, The Netherlands), pp. 58–69.

Lin, T., and Guinan, J. J., Jr. (**2000**). ''Auditory-nerve-fiber responses to high-level clicks: Interference patterns indicate that excitation is due to the combination of multiple drives,'' J. Acoust. Soc. Am. **107**, 2615–2630.

Lutfi, R. A., and Patterson, R. D. (**1984**). ''On the growth of masking asymmetry with stimulus intensity,'' J. Acoust. Soc. Am. **76**, 739–745.

Lyon, R. F. (**1996**). ''The all-pole gammatone filter and auditory models,'' Forum Acusticum '96, Antwerp, Belgium.

Lyon, R. F. (**1997**). ''All-pole models of auditory filtering,'' in *Diversity in Auditory Mechanics*, edited by Lewis, E. R., *et al.* (World Scientific, Singapore).

Moore, B. C. J., and Glasberg, B. R. (**1987**). ''Formulae describing frequency selectivity as a function of frequency and level, and their use in calculating excitation patterns,'' Hear. Res. **28**, 209–225.

Moore, B. C. J., Peters, R. W., and Glasberg, B. R. (**1990**). ''Auditory filter shapes at low center frequencies,'' J. Acoust. Soc. Am. **88**, 132–140.

Møller, A. R., and Nilsson, H. G. (**1979**). ''Inner ear impulse response and basilar membrane modelling,'' Acustica **41**, 258–262.

Oxenham, A. J., and Plack, C. J. (**1997**). ''A behavioral measure of basilar-membrane nonlinearity in listeners with normal and impaired hearing,'' J. Acoust. Soc. Am. **101**, 3666–3675.

Patterson, R. D. (**1974**). ''Auditory filter shape,'' J. Acoust. Soc. Am. **55**, 802–809.

Patterson, R. D. (**1976**). ''Auditory filter shapes derived with noise stimuli,'' J. Acoust. Soc. Am. **59**, 640–654.

Patterson, R. D., and Moore, B. C. J. (**1986**). ''Auditory filters and excitation patterns as representations of frequency resolution,'' in *Frequency Selectivity in Hearing*, edited by Moore, B. C. J. (Academic Press, London), pp. 123–177.

Patterson, R. D., and Nimmo-Smith, I. (**1980**). ''Off-frequency listening and auditory-filter asymmetry.'' J. Acoust. Soc. Am. **67**, 229–245.

Patterson, R. D., Allerhand, M., and Giguère, C. (**1995**). ''Time-domain modelling of peripheral auditory processing: a modular architecture and a software platform,'' J. Acoust. Soc. Am. **98**, 1890–1894.

Patterson, R. D., Nimmo-Smith, I., Weber, D. L., and Milroy, R. (**1982**). ''The deterioration of hearing with age: Frequency selectivity, the critical ratio, the audiogram, and speech threshold,'' J. Acoust. Soc. Am. **72**, 1788–1803.

Patterson, R. D., Robinson, K., Holdsworth, J. W., McKeown, D., Zhang, C., and Allerhand, M. (**1992**). ''Complex sounds and auditory images,'' in *Auditory Physiology and Perception*, edited by Cazals, Y., Demany, L. and Horner, K. (Pergamon, Oxford), 429–446.

Patuzzi, R., and Robertson, D. (**1988**). ''Tuning in the mammalian cochlea,'' Physiol. Rev. **68**, 1009–1081.

Pickles, J. O. (**1988**). *An Introduction to the Physiology of Hearing* (Academic, London).

Press, W. H., Flannery, B. P., Teukolsky, S. A., and Vetterling, W. T. (**1988**). *Numerical Recipes in C* (Cambridge U. P., Cambridge).

Recio, A. R., Rich, N. C., Narayan, S. S., and Ruggero, M. A. (**1998**). ''Basilar-membrane response to clicks at the base of the chinchilla cochlea,'' J. Acoust. Soc. Am. **103**, 1972–1989.

Rose, S., and Baker, R. J. (**1994**). ''Characterising auditory filter nonlinearity,'' Hear. Res. **73**, 231–243.

Ruggero, M. A. (**1992**). ''Responses to sound of the basilar membrane of the mammalian cochlea,'' Curr. Opin. Neurobiol. **2**, 449–456.
Ruggero, M. A., Rich, N. C., Recio, A. R., Narayan, S. S., Robles, L. (**1997**). ''Basilar-membrane response to tones at the base of the chinchilla cochlea,'' J. Acoust. Soc. Am. **101**, 2151–2163.
Schofield, D. (**1985**). ''Visualizations of speech based on a model of the peripheral auditory system,'' NPL Report DITC 62/85.
Slaney, M. (**1993**). ''An efficient implementation of the Patterson-Holdsworth auditory filterbank,'' Apple Computer Technical Report #35.